

REPORT DOCUMENTATION PAGE

AFRL-SR-AR-TR-02-

0375

Public Reporting burden for this collection of information is estimated to average 1 hour per response, including the time for gathering and maintaining the data needed, and completing and reviewing the collection of information. Send comment regarding this burden estimate or any aspect of this collection of information, including suggestions for reducing this burden, to Washington Headquarters Services, Directorate for Information Operations and Reports, 1215 Jefferson Davis Highway, Suite 1204, Arlington, VA 22202-4302, and to the Office of Management and Budget, Paperwork Reduction Project (0704-0188), Washington, DC 20503.

1. AGENCY USE ONLY (Leave Blank)		2. REPORT DATE 03/01/01 - 05/31/02	3. REPORT TYPE AND DATES COVERED Final Technical	
4. TITLE AND SUBTITLE Pressure Transducer and Computer System Providing Instantaneous Information Over a Surface and Time-Dependent Predictive Ability			5. FUNDING NUMBERS F49620-01-1-0249	
6. AUTHOR(S) Israel Wagnanski				
7. PERFORMING ORGANIZATION NAME(S) AND ADDRESS(ES) Department of Aerospace and Mechanical Engineering The College of Engineering and Mines - The University of Arizona Tucson, AZ 85721			8. PERFORMING ORGANIZATION REPORT NUMBER	
9. SPONSORING / MONITORING AGENCY NAME(S) AND ADDRESS(ES) AFOSR/NA 801 N. Randolph St. Room 732 Arlington, VA 22203-1977			10. SPONSORING / MONITORING AGENCY REPORT NUMBER	
11. SUPPLEMENTARY NOTES				
12 a. DISTRIBUTION / AVAILABILITY STATEMENT Approved for public release; distribution unlimited.			12 b. DISTRIBUTION CODE	
13. A PSI 8400 pressure transducer system providing mean pressures almost instantaneously out of 48 ports and capable of responding to low frequency oscillations was purchased and absorbed by the laboratory in support of the various separation control investigations. An array of 64 Endevco surface mounted transducers capable of dynamic measurements of pressure oscillations were also bought together with National Instruments signal conditioner units. These were already used in monitoring pressure oscillations in a cavity that were generated by actuators used on wings of the XV-15 and V-22 models for the purpose of download alleviation. Four powerful PC computers and a server were purchased for data acquisition and storage, as well as for LES computations supporting the experiments being carried out in the Aerodynamic Laboratories at the University of Arizona.				
14. SUBJECT TERMS			15. NUMBER OF PAGES 10	
			16. PRICE CODE	
17. SECURITY CLASSIFICATION OR REPORT UNCLASSIFIED	18. SECURITY CLASSIFICATION ON THIS PAGE UNCLASSIFIED	19. SECURITY CLASSIFICATION OF ABSTRACT UNCLASSIFIED	20. LIMITATION OF ABSTRACT UL	

NSN 7540-01-280-5500

Standard Form 298 (Rev.2-89)
Prescribed by ANSI Std. Z39-18
298-102

20021126 038

August 16, 2002

**PRESSURE TRANSDUCER AND COMPUTER SYSTEM
PROVIDING INSTANTANEOUS INFORMATION OVER A SURFACE
AND TIME-DEPENDENT PREDICTIVE ABILITY.**

Final Report on DURIP Grant Number F496200110249

Submitted to AFOSR

AUGUST 2002

I.WYGNANSKI

Aerospace and Mechanical Engineering Department

The University of Arizona

Tucson, AZ, 85721

PROJECT SUMMARY

A PSI 8400 pressure transducer system providing mean pressures almost instantaneously out of 48 ports and capable of responding to low frequency oscillations was purchased and absorbed by the laboratory in support of the various separation control investigations. An array of 64 Endeveco surface mounted transducers capable of dynamic measurements of pressure oscillations were also bought together with National Instruments signal conditioner units. These were already used in monitoring pressure oscillations in a cavity that were generated by actuators used on wings of the XV-15 and V-22 models for the purpose of download alleviation. Four powerful PC computers and a server were purchased for data acquisition and storage, as well as for LES computations supporting the experiments being carried out in the Aerodynamic Laboratories at the University of Arizona.

Actuator Calibration Procedure Using Endevco Sensors and a Hot-Wire Anemometer

The calibration procedure begins by mapping the performance of the actuators in use with the XV-15 wing model. The procedure for the calibration was maintained consistent using an apparatus specifically developed to test actuation performance. The wing or airfoil is held on an optical table outside a wind tunnel where a traversing mechanism enables an insertion of a hot wire into a small slot with precision. A constant temperature hot-wire anemometer, with a single wire probe, was calibrated against a standard pitot-static pressure probe. A fourth order polynomial, obtained from a least squares curve fit, was used to characterize the relationship between velocity and the anemometer bridge potential. Thereafter, all measurements were taken using a hot wire that was inserted into the middle of the slot and only occasionally was traversed across the slot's width to establish the departure of the velocity profile from a "top-hat" shape. The hot wire was inserted into the slot. At this position the velocity time-trace from the anemometer looks symmetric and uniform when viewed through an oscilloscope. This indicates that the anemometer is equally sensitive to both the in (suction) and out (blowing) stroke of the actuator and that the probe is correctly positioned. One-second velocity data was sampled to provide time series that were then acquired at a 5kHz sample rate. All frequency sweeps of the actuation were made going from a lower frequency to a higher one.

The Necessity of Monitoring Internal Pressure Perturbations

In conjunction with hot wire measurements of the velocity of the jet emanating from the slot, the dynamic pressure inside the actuator cavity was also measured. This measurement is both an informative and necessary component of the calibration of the model. Endevco transducers were mounted into the internal cavities of the model at various positions along the span corresponding to the presence of individual actuators. The presence of this type of transducer allows us to monitor the internal pressures with changing frequency and input voltage to the actuator. Thus, we can construct a matrix relating these values to a certain jet velocity and from it the momentum coefficient, C_{μ} . This is a necessary addition to the calibration procedure due to the absence of outside flow during the calibration procedure. When the airfoil is placed in the wind

tunnel, the flow along the outside of the model can reduce the pressure outside the slot. This sometimes affects the performance of the actuator and does not allow a direct transference from the calibration table to the test situation. This means that a certain input voltage and frequency on the calibration table does not correlate to the same velocity output in the tunnel. However, by setting the actuator to comparative internal pressure oscillations, a correct monitoring of the jet output can be maintained in the test setup. Furthermore, it enables us to monitor any deterioration in the actuator performance throughout the test. Some representative data is provided in the figures below. This method applies not only to the XV-15 model, but also to other wings, airfoils and even bluff body models that have been calibrated using the same procedure.

The cavity pressure fluctuations resulting from a constant voltage input to the actuator at various frequencies are presented in Figure (1). It is clear that differences equivalent to an order of magnitude in the output may result by selecting the proper cavity that responds well to the needed fluctuations. In this case the cavity resonates at 125Hz and at 225Hz.

In Figure (2) a comparison is made between the hot wire in situ calibration and the reading from the calibrated pressure transducer for a variety of input amplitudes at a given frequency. The spectral analysis of the pressure fluctuation inside a cavity, when an actuator is operating, is shown in Figure (3). Usually when an actuator is about to fail or become dysfunctional in any manner, it generates odd noises that can be best observed by watching the signal emitted from the pressure transducer and its spectrum. Therefore, the pressure transducer serves as a health monitoring system.

Comparison Between C_{μ} and Internal Pressure
for 24 Vrms Input for XV-15

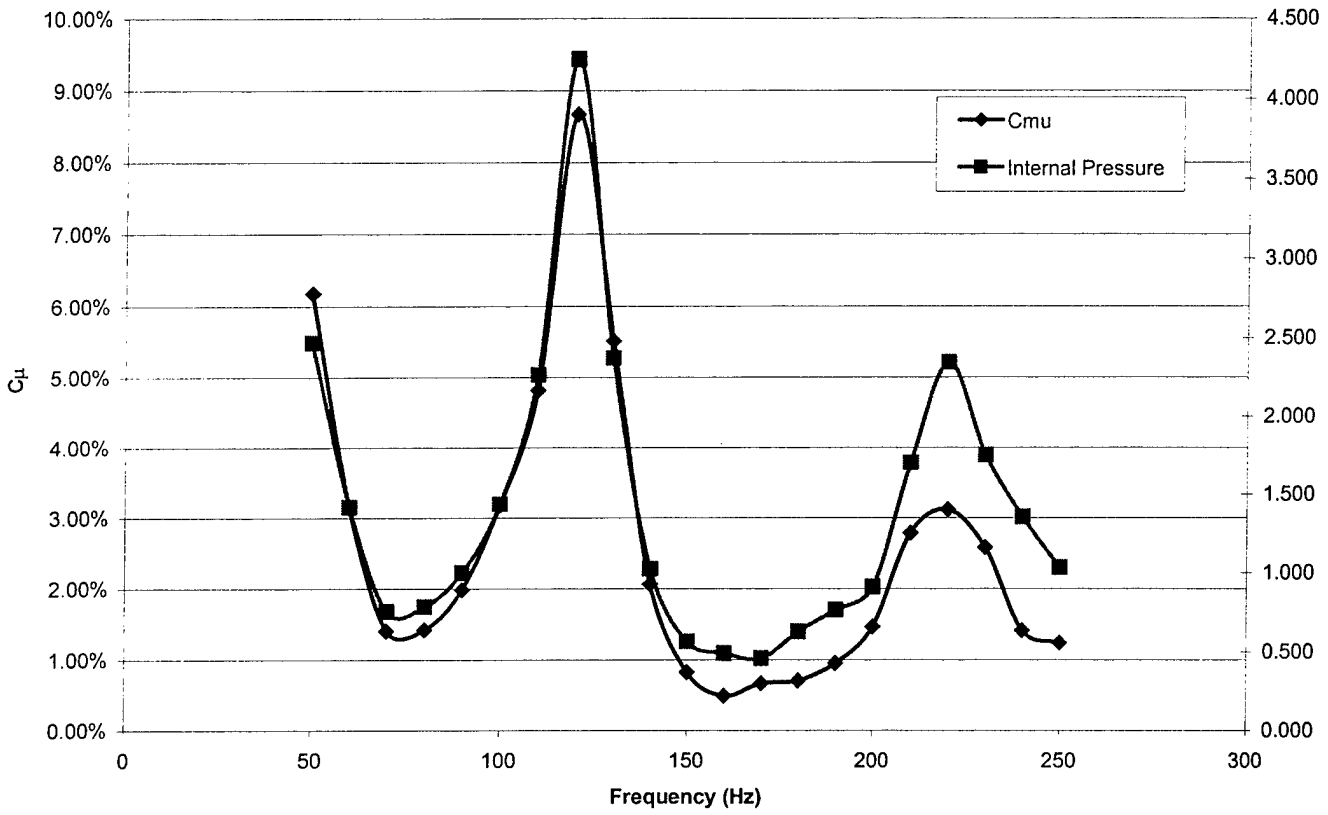


Figure 1.

Comparison Between C_{μ} and Internal Pressure
for Constant Frequency on the Cylinder Model

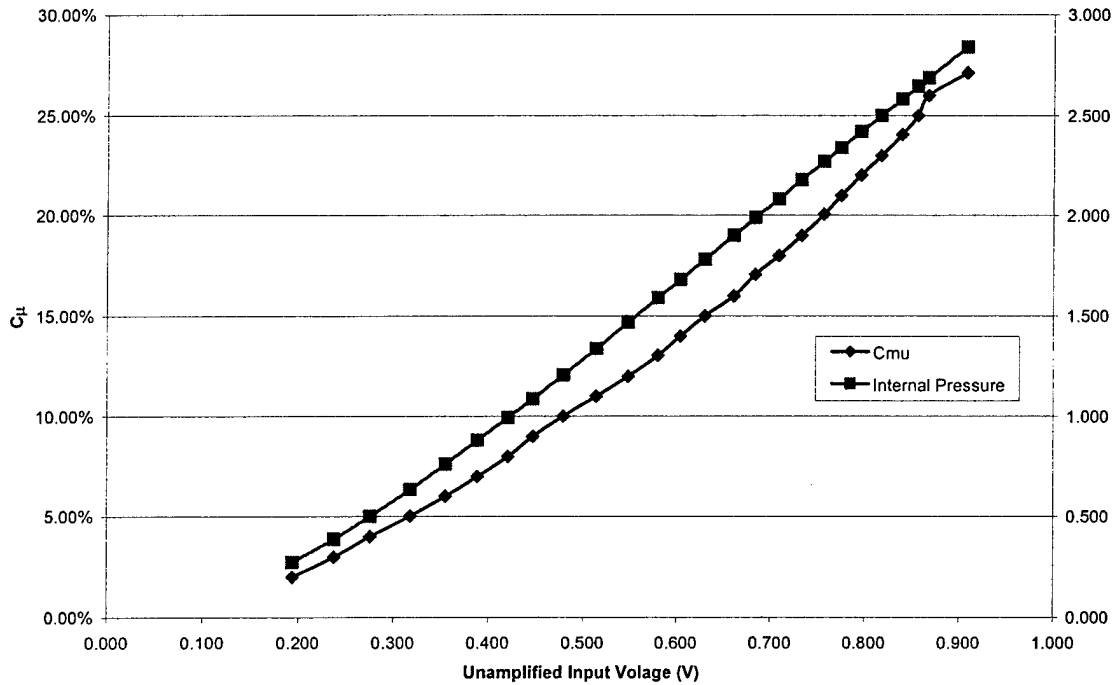


Figure 2.

**Spectral Analysis at 100 Hz and 5% Cu
Internal Pressure Data Used for Cylinder Model**

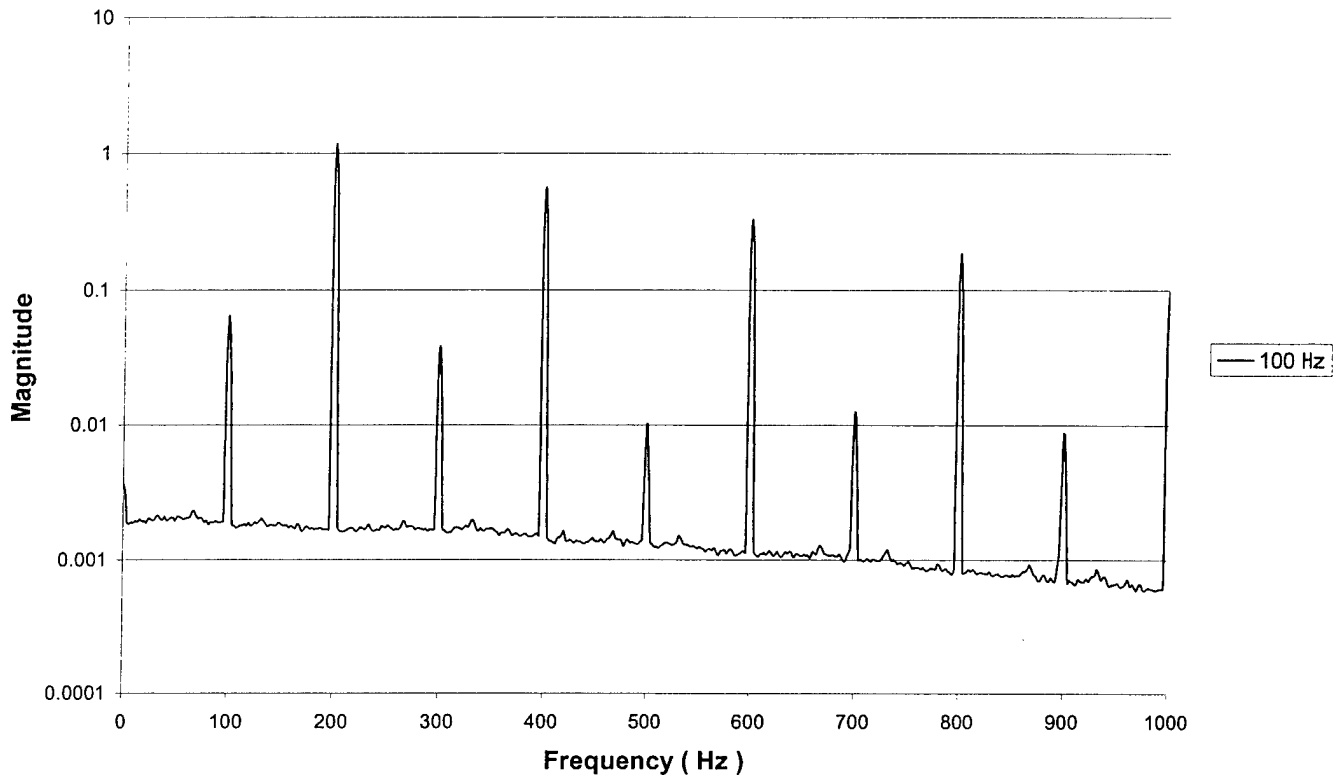
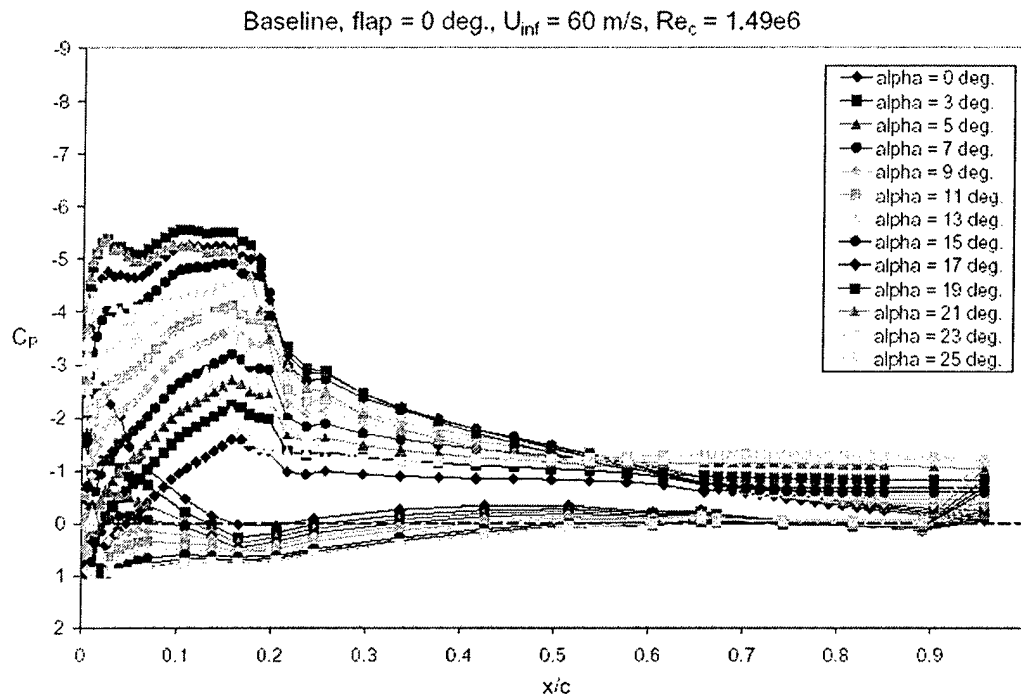


Figure 3.

The Measurement of Pressure Distribution on Airfoils using the PSI 8400 System

The use of active separation control techniques on airfoils requires a very large number of measurements due to the increased number of parameters to be investigated. A rapid acquisition of pressures is important in this case. Integral parameters, like lift coefficient C_L obtained by using a sting balance, do not provide sufficient information about the flow and can not guide the investigator as to the required step to be taken to prevent impending separation. An example of the pressure distribution on a typical flapped airfoil taken by using the newly acquired PSI system is shown in Figure (4). In this case the flap is not deflected, but the flow starts to separate from the trailing edge of the airfoil when the incidence angle, α , exceeds 7° .



The Use of PC's for Time-dependent Large Eddy Simulations

Computer simulations have proved to be of great importance, since they provide a means of cheaper and faster information about design changes and their effect on the fluid flow. Five to six personal computers are constantly used to provide simulations addressing various problems that might result in design changes associated with the use of active flow control on airfoils. In the attached example, calculations were performed for various download configurations related to tilt-rotor aircraft using the V-22 and the XV-15 airfoil geometry. Since the calculations for these are carried out in a similar fashion, the numerical issues will be discussed in more detail for the XV-15 airfoil, but results for both will be shown.

A Large Eddy Simulation (LES) is always three-dimensional and time-dependent. For the cases shown here, the size of the computational domain is typically $20 \times 15 \times 0.3$ chords. The height of the domain, 15 chords, should be large enough to make the blockage insignificant. There was no blockage in the experiment, since the wind tunnel side walls were removed. The width in the spanwise direction is set to 0.3 chords. Obviously, this is not large enough to include all scales in the wake; and it is likely that the computed flow is less three-dimensional than reality. However, it is believed that it is large enough to capture the main characteristics of the flow

adequately. It was chosen in that way so that a good spanwise resolution can be achieved with a relatively small number of nodes. Furthermore, because it is not large enough to be able to use periodic boundary conditions that are so popular in LES, slip-walls are used as boundary conditions. The small width in the spanwise direction reduces the computational requirements, but likely causes the flow to have too little three dimensionalities. A schematic view of the computational domain is shown in Figure (5).

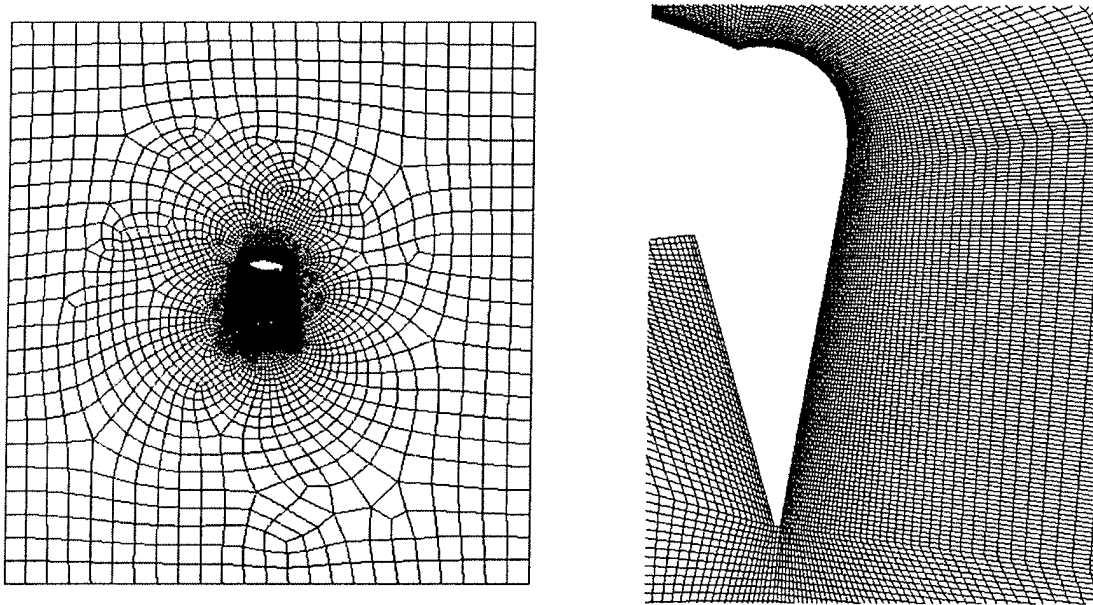


Figure 5. Computational mesh around the XV-15 airfoil and flap

The ability of the unstructured mesh allows the nodes to be heavily concentrated in the boundary layer and in the near-wake region, as is shown in Figure (5).

The number of nodes is approximately 300,000-700,000 and typically 100,000 time steps are used. The time step varies throughout the calculation, changing every tenth time step by an automatic time stepper that keeps the Courant number constant. Typically, the Courant number was set in the range of 1.5 – 2.0. Notice that a Von Neumann linear stability analysis requires Courant number < 2.8 for a lumped mass matrix and < 1.6 for a consistent mass matrix in one dimension. When doing actual calculations, it was found that a Courant number as high as even 5 to 10 would still keep the calculation stable. However, it seemed risky. Furthermore, larger time

steps lead to more iterations for the pressure Poisson solver and may also be too large for the development of turbulence [10]. The actual size of the time step used was approximately 2×10^{-5} to 1×10^{-4} seconds.

The following steps were conducted for every configuration to carry out the calculations:

- i) Calculate two-dimensional low Reynolds number flow so that boundary layers, vortex shedding etc. are well developed.
- ii) Extend the two-dimensional mesh to three-dimensional by extruding in the z-direction. Use the results from the two-dimensional calculations, with an added perturbation of 1%, as initial condition for the three-dimensional calculation. Calculate the unforced case.
- iii) Use result from the unforced case as initial condition. Add forcing by applying time-dependent Dirichlet conditions at the slot location.

Because the forced calculations are always started using the unforced calculations, the flow will not be attached prior to the forcing. The experiments were conducted in a similar fashion to compare results eliminating any hysteresis effect. LES calculations shown in Figure (6) were performed for the V-22 airfoil configurations $\alpha = -85^\circ$ and $\delta_f = 80^\circ$, and $\alpha = -85^\circ$ and $\delta_f = 75^\circ$. The LES calculations for the XV-15 airfoil were at $\alpha = -85^\circ$ and $\delta_f = 80^\circ$.

The computational results help to explain what is going on in the flow field to cause large changes in drag. They provide also a time history of the airfoil's drag coefficient that is almost impossible to get experimentally. Some four seconds after the starting of forcing, a rapid drop in the drag coefficient occurs. Large fluctuations in the drag coefficient are present, particularly for the unforced condition where the peak-to-peak value is greater than unity. An example of the pressure flow field contours is shown in Figures (6a). The cause of the maximum transient drag coefficient is the negative pressure created on the lower part of the airfoil by the large global vortices shed from the leading and the trailing edges.

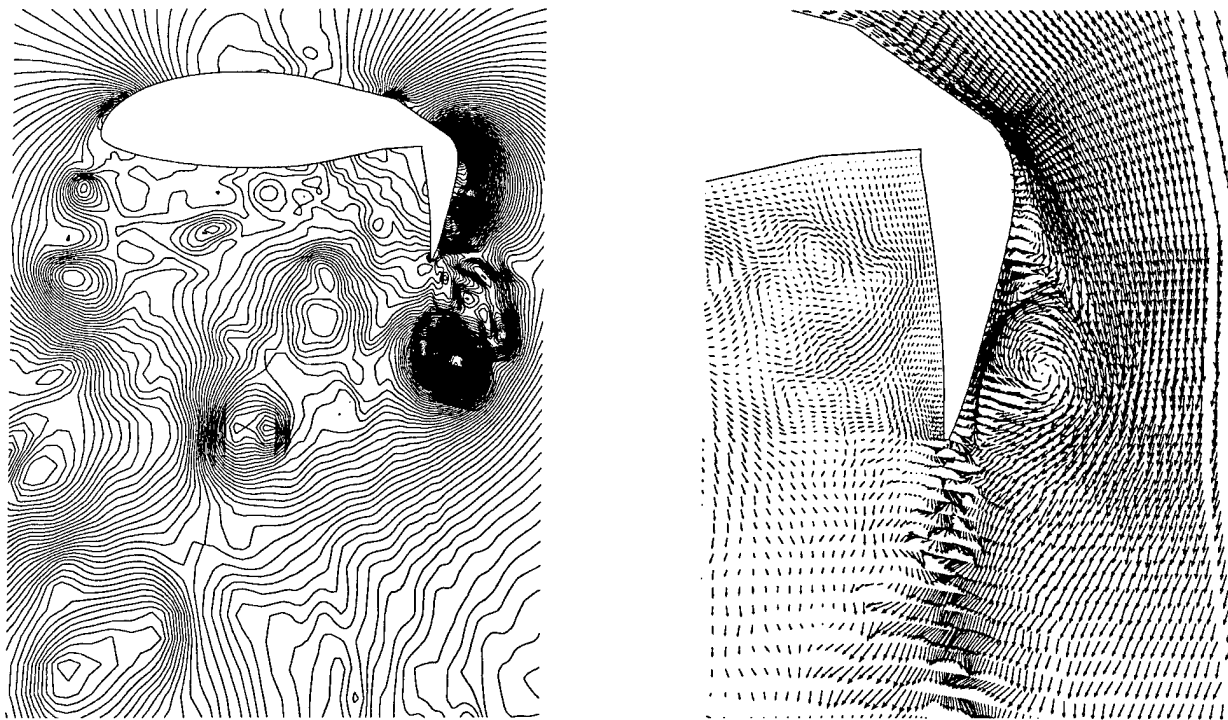


Figure 6. Instantaneous pressure and velocity fields. From three-dimensional time-dependent LES at $Re=130,000$. a) Pressure field around airfoil. b) Velocity vector field around the flap.

Very little AFC input is required to cause an immediate drag reduction, eliminating the very large structures in the wake. More activation energy is required as larger drag reduction is sought, breaking the wake structures into smaller and smaller vortices.

From the practical aspect, the computations enable one to decide about the optimal actuation location that provides the minimum download for a given configuration. The dependence of the download on the slot location is shown in Figure (7) where the computational results are compared to experiment.

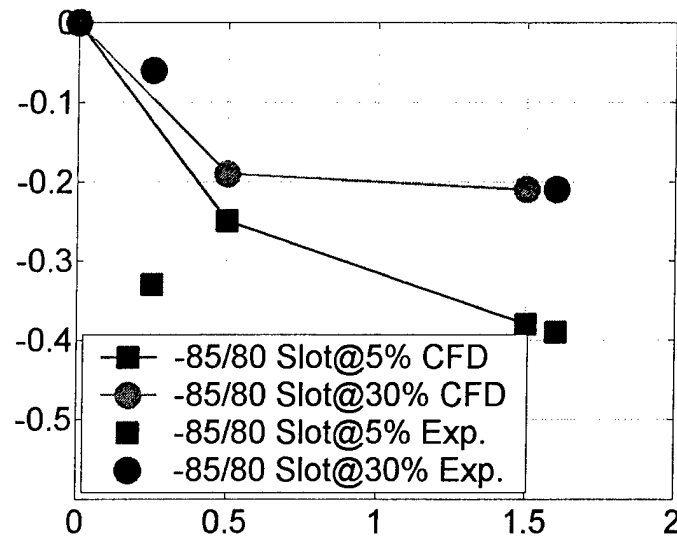


Figure 7. V-22 airfoil download, drag reduction as function of forcing. $U=7$ m/s, forcing freq.=61 Hz, slot location 5% and 30% of flap chord. Slot width=1 mm. Flap deflection angle 80 degrees.

Conclusion

The purchase of the equipment purchased with DURIP funds enabled us to improve our data acquisition and computational ability. The equipment is currently used in support of DARPA project on download alleviation on the XV 15 and V-22 airplanes